Hindawi
Shock and Vibration
Volume 2022, Article ID 7012510, 12 pages
https://doi.org/10.1155/2022/7012510

Research Article

Experimental and Numerical Studies on Bond Quality of Fully Grouted Rockbolt under Confining Pressure and Pull-Out Load

Shuisheng Yu,[1,2] **Leilei Niu**,[2] **and Jin Chen**[3]

[1]*School of Architectural Engineering, Zhongyuan University of Technology, Zhengzhou 450007, China*
[2]*Center for Rock Instability and Seismicity Research, Department of Mining Engineering, School of Resource and Civil Engineering, Northeastern University, Shenyang 110819, China*
[3]*School of Economics and Management, Zhongyuan University of Technology, Zhengzhou 450007, China*

Correspondence should be addressed to Shuisheng Yu; yuss.1987@163.com

Received 11 June 2022; Accepted 12 July 2022; Published 25 August 2022

Academic Editor: Amr A. Nassr

In mining engineering, the *in situ* stress changes with the stress induced by the surrounding mining activities. It positively or negatively affects the propagation of ultrasonic guided waves in rockbolts. Therefore, the effect of *in situ* stress in rockbolt support was determined by applying confining pressure and pull-out load in a laboratory test and using ultrasonic guided waves to test the rockbolt. Furthermore, the propagation law of ultrasonic guided waves and bond quality of the rockbolt under the interaction of the pull-out load and confining pressure were studied. Numerical simulations were performed to deduce the guided wave propagation process in grouted systems, and the influencing mechanism of the pull-out load and confining pressure on the guided wave propagation was discussed. The laboratory test and numerical simulation results show that the confining pressure weakens the guided wave propagation without pull-out load. Under the same pull-out load, the guided wave propagation gradually strengthens with increasing confining pressure. A larger confining pressure weakens the weakening effect of the pull-out load and suppresses the discreteness of the guided wave propagation. Under the same confining pressure, the guided waves did not diffract well into the cement mortar and concrete with increasing pull-out load, the confining pressure restricted the radial vibration of the guided waves, and the guided wave propagation law weakened. Thus, the pull-out load plays a weakening role in the propagation law of ultrasonic guided waves.

1. Introduction

In mining engineering, the magnitude and direction of *in situ* stress are the key factors that affect the stability of the surrounding rock in bolt-supported roadways. However, during the actual construction of the rockbolt, construction quality problems are unavoidably encountered, such as the debonding between the rockbolt and grouted agent [1], insufficient length of the rockbolt [2], and corrosion [3–5]. Furthermore, the stability and safety of the rockbolt supporting structure are always affected by natural joints [6–8].

In order to ensure the stability and safety of the supporting structure, accidents of the supporting structure need to be avoided, the service life of the supporting structure needs to be prolonged, and the reliability of the supporting structure needs to be improved. Scholars [9–14] used nondestructive testing methods to test the bond quality of rockbolts. Zou et al. [9] used ultrasonic guided waves to study the bond quality of rockbolts in terms of their group velocity and attenuation and considered the effect of mortar strength and air content on the bond quality. Madenga et al. [10] used ultrasonic guided waves to study the effect of curing time, frequency, and bond length on the velocity of ultrasonic guided waves in rockbolts. Additionally, Lee et al. [11] used Fourier transform and wavelet analysis to analyze the bond quality of rockbolts and compared the results with the test results, showing that the bond quality of rockbolts can be tested. Yu et al. [12] used the ultrasonic guided wave reflection method to evaluate the unanchored ratio of rockbolts in three different states, conducted wavelet

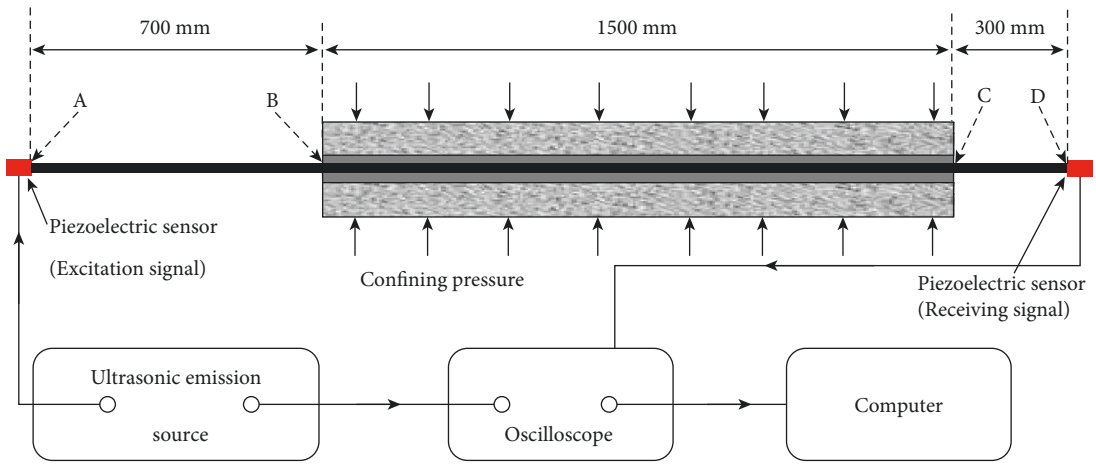

Figure 1: Grouted rockbolt systems model.

transform on the test data, and stated that the length of the unanchored section of a rockbolt could be detected using ultrasonic guided waves. Beard and Lowe [13] used a numerical simulation method to determine the affected range of the rockbolt attenuation at low and high frequencies. They analyzed the effect of the rock elastic modulus, the bond agent elastic modulus and thickness, and the interface quality of the rockbolt/bond agent on wave attenuation. Cui and Zou [14] studied the attenuation and group velocity of ultrasonic guided waves in rockbolts and confirmed the effect of insufficient rockbolts and lack of mortar on rockbolts for bonding.

During the service period, rockbolts often experience three-dimensional stress, and the bond quality of rockbolts is always affected by the pull-out load and confining pressure [15]. Rizzo [16] stated that the attenuation characteristics of materials were constantly under stress, but the ultrasonic velocity was variable. Chen and Wilcox [17] analyzed the effect of load on the guided wave and determined that the phase velocity of the guided wave increased with the increasing load, but the group velocity decreased. Kwun et al. [18] and Chen and Wissawapaisal [19, 20] studied the influence of tensile load on the propagation of axial modal elastic waves in seven-strand steel cables and determined that some of the frequency components of the stress waves became highly attenuated. Liu et al. [21] analyzed the effect of tensile stress on the propagation properties of ultrasonic guided waves in steel cables based on fast Fourier transforms and found that the energy transfer of ultrasonic guided waves increased with the pull-out load.

In summary, although some scholars have studied the properties of ultrasonic guided waves in steel cables under different stress levels, they have not considered whether the rockbolt is debonded, the debonding length and the propagation process of ultrasonic guided waves in grouted rockbolt systems due to the propagation, reflection, and diffraction of waves. Furthermore, they have only considered the action of pull-out loads but not the action of the confining pressure. Therefore, in view of the above issues, the bond quality of rockbolts tested with ultrasonic guided waves under different triaxial loadings (confining pressure and pull-out load) was analyzed to quantify the debonding length of the rockbolts under pull-out load and determine the bond quality of the rockbolts. Moreover, a numerical simulation method was employed to deduce the ultrasonic guided waves propagating process in grouted rockbolt systems.

2. Test Design

2.1. Specimen Design. Ribbed rockbolts with a diameter of 25 mm and a length of 2,500 mm were used, and the rock mass intended for reinforcement was simulated with a hollow cylinder composed of concrete. The diameter and length of the hollow cylinder were 150 and 1500 mm, respectively. The embedment length of the rockbolt was 1500 mm. Figure 1 presents the details of the testing sample preparation.

The specimen was a hollow cylinder composed of C40 concrete, which comprised (1) ordinary Portland cement with a standard 28-day compressive strength of 42.5 MPa; (2) tap water; (3) natural river sand (the main ingredient is silica) fine aggregates with diameters ranging from 0.3 to 1.18 mm; and (4) cobblestone coarse aggregates with diameters ranging from 5 to 20 mm, and was mixed at a ratio of 1 : 0.47 : 1.3 : 3.02.

The grout was a cement-based mixture comprising (1) ordinary Portland cement with a standard 28-day compressive strength of 42.5 MPa; (2) tap water; and (3) natural river sand (the main ingredient is silica) fine aggregates with diameters ranging from 0.3 to 0.6 mm. Table 1 lists the mixing proportions of the cement mortar and concrete [22].

2.2. Test Procedure. The Pull-out Testing Machine (PTM) was designed and manufactured to conduct the rockbolt pull-out test with the monitoring of the stress wave propagation in the rockbolt [22]. The pull-out load was applied to the rockbolt using a hollow Jack with a 300 kN loading capacity. Figure 1 displays the schematic of the grouted rockbolt systems. Piezoelectric sensors (TH-GP) and ultrasonic emission sources (TH-F) were produced by

Table 1: Mix proportions of concrete and cement mortar in the test.

Ingredient	Water	Cement	Sand	Stone
Concrete	0.47	1	1.3	3.02
Cement mortar	1	1	3.2	0

Xiangtan Tianhong Testing Technology Co., Ltd. (China). The emission voltages of the ultrasonic emission source were 100–1,000 V. A piezoelectric sensor was employed as the receiving or excitation sensor, which could excite 10-cycle sine wave packets with a main frequency of 22 kHz. An ultrasonic excitation sensor was placed in contact with the loading end (A-end in Figure 1) of the rockbolt using a coupling agent (such as Vaseline) to generate signals, which were received at the free end (D-end in Figure 1) of the rockbolt by the receiving sensor.

The testing procedure was as follows: first, the grouted rockbolt was maintained without the pull-out force and confining pressure; the ultrasonic excitation sensor was used to excite the ultrasonic guided wave at the A-end, and the receiving sensor at the D-end received the wave. Next, 2 MPa confining pressure was applied, and the bolt was detected by ultrasonic waves in the absence of pull-out load. Then, the confining pressure was kept constant, the pull-out load was increased to 80 kN, and the above steps were repeated. Finally, the rockbolt was pulled until it was completely debonded from the concrete specimen, and the ultrasonic guided wave was tested according to the above steps. Based on the results of ultrasonic guided wave testing, the bond quality of the rockbolt under the combined action of pull-out load and confining pressure was analyzed.

3. Experimental Results and Discussion

3.1. Effect of Confining Pressure on Guided Wave Propagation without Pull-Out Load. The frequency information of an ultrasonic guided wave signal is extremely important for its propagation in a rockbolt. Therefore, the Fourier transform was employed to analyze the frequency domain characteristics of the received signals. Using Fourier transform, the signals were decomposed into spectra with different frequencies. The Fourier transform is the integral of $f(t)$ from $t = -\infty$ to $+\infty$:

$$F(\omega) = \int_{-\infty}^{+\infty} f(t) e^{-i\omega t} \mathrm{d}t, \quad (1)$$

where $F(\omega)$ is the Fourier transform of $f(t)$, i is $\sqrt{-1}$, and the frequency variable ω is the angular frequency.

As shown in Figure 2, the guided wave is propagated at confining pressures of 0 and 2 MPa in the absence of pull-out load. Figure 2 shows that regardless of whether the bond system is subjected to the confining pressure, the echoes of the A- and B-end of the bond system can be simultaneously received at the D-end of the rockbolt. However, the guided wave waveform under a confining pressure of 2 MPa is somewhat disordered compared to that under no confining pressure. The above phenomenon denotes that the velocity of a guided wave does not change under the action of the

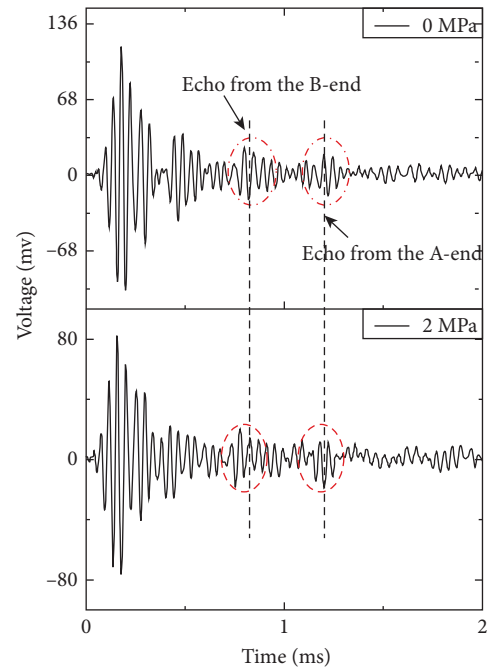

Figure 2: The guided wave received at D-end under different confining pressures in the absence of pull-out load.

confining pressure. However, owing to the confining pressure, the concrete becomes "harder," the cement mortar and rockbolt are closely bonded, the bond quality of the rockbolt is strengthened and the natural frequency of the lateral vibration of the rockbolt is increased [23]. Thus, the confining pressure restricts the vibration of guided waves in the propagation process, weakens the propagation law, and has a weakening effect. The frequency domain of the guided wave in Figure 3 shows that when the confining pressure is increased to 2 MPa from 0 MPa, the ratio Q of the maximum amplitude of the guided wave at low frequency to that at high-frequency increases from 0.086 to 0.215. In other words, the low-frequency increases and the guided wave frequency shifts from high frequency to low frequency, which weakens the guided wave propagation law.

3.2. The Effect of Pull-Out Load on Guided Wave Propagation under 2 MPa Confining Pressure. Figure 4 displays the signals detected under different pull-out loads when the confining pressure is 2 MPa. The echoes of the B- and A-end of the grouted systems were received at the D-end of the rockbolt when the pull-out load was 0 kN. Based on the guided wave propagation velocity in the free rockbolt and the echo time of the A-end received at the D-end, the guided wave velocity in the rockbolt of the grouted section was 4,145 m/s. However, after the rockbolt was completely debonded, the propagation velocity in the rockbolt in the grouted section was 4,854 m/s according to the transiting time. Based on the wave velocity of the guided wave in the rockbolt, when the pull-out load was 0 kN and the rockbolt was completely debonded, the length of the debonded bolt under the action of a confining pressure of 2 MPa and a pull-

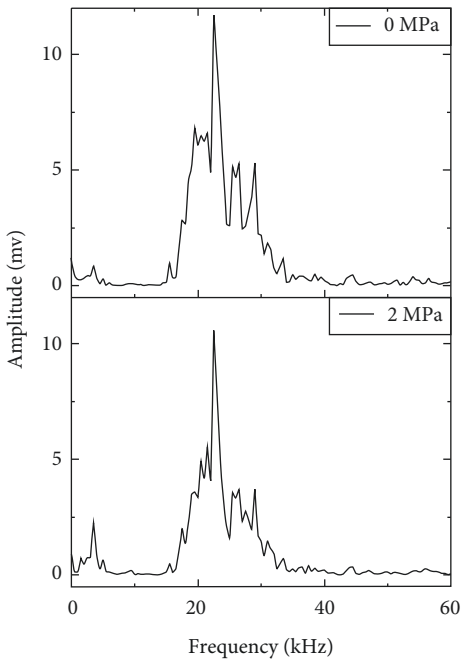

Figure 3: The frequency domain under different confining pressures in the absence of pull-out load.

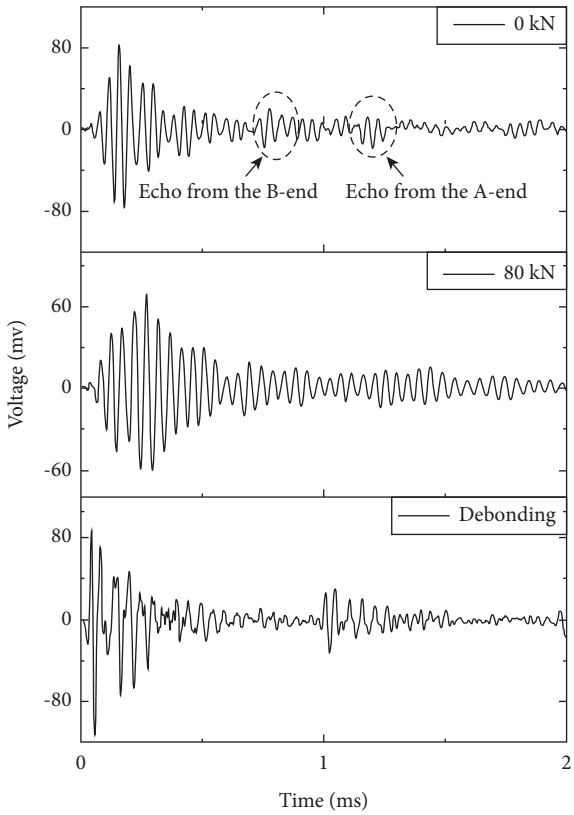

Figure 4: The guided wave received at D-end under different pull-out loads with 2 MPa confining pressure.

out load of 80 kN was 198 mm, accounting for 13.2% of the total bond length. Although the bond quality was relatively reduced, the rockbolt did not yield or harden and still

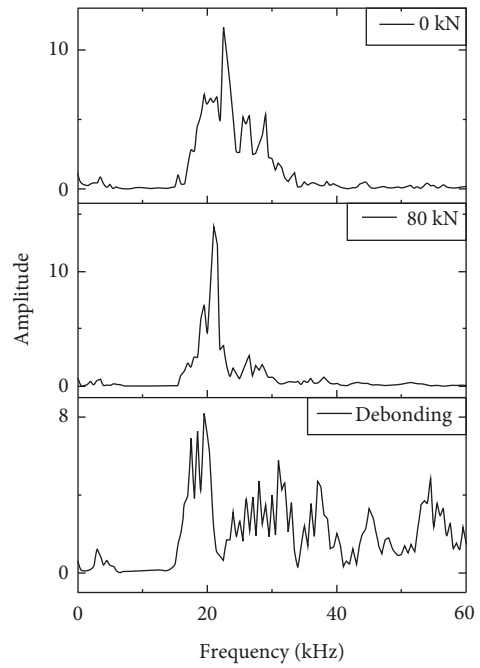

Figure 5: The frequency domain of guided wave under different pull-out loads with 2 MPa confining pressure.

afforded the maximum bearing capacity. When the pull-out load was 80 kN, the average wave velocity of the guided wave in the rockbolt was 4,573 m/s.

Figure 5 displays the guided wave frequency domain under different loads when the confining pressure is 2 MPa. When the pull-out load is increased from 0 to 80 kN and the rockbolt is completely debonded, the main frequency of the guided wave signal slightly decreases and shifts to 22.6, 21, and 19.8 kHz, which was mainly caused by damage to the grouted rockbolt systems [24]. This phenomenon is consistent with the results obtained by [25].

4. Numerical Analysis of the Bond Quality of Rockbolt under Pull-Out Load and Confining Pressure

The concrete damage plasticity model (CDPM) employed herein to simulate the mechanical behavior of quasi-brittle materials (concrete and cement mortar) was proposed for introduction to Abaqus by Lee and Fenves [26]. CDPM considers isotropic damaged elasticity in combination with isotropic tensile and compressive plasticity to represent the inelastic behavior of concrete [27]. The model has the advantage of simplicity and numerical stability [28, 29].

In the numerical model, grouted rockbolt systems are simulated by four-node bilinear axisymmetric quadrilateral elements with reduced integration (CAX4R). A two-dimensional axisymmetric model, whose effectiveness has been verified by Yu et al. [22], was used to simulate the debonding process of the rockbolts. The interface at the loaded end of the concrete was fixed during the test for the boundary condition in the rockbolt-grouted system. Based on extensive trials, mesh sizes of 2 mm for the rockbolt and

Table 2: Material properties of the rockbolt, concrete, and cement mortar.

Ingredient	Density (kg/m^3)	Elastic modulus (GPa)	Poisson's ratio
Rockbolt	7850	210	0.3
Cement mortar	2035	15.3	0.16
Concrete	2300	33	0.23

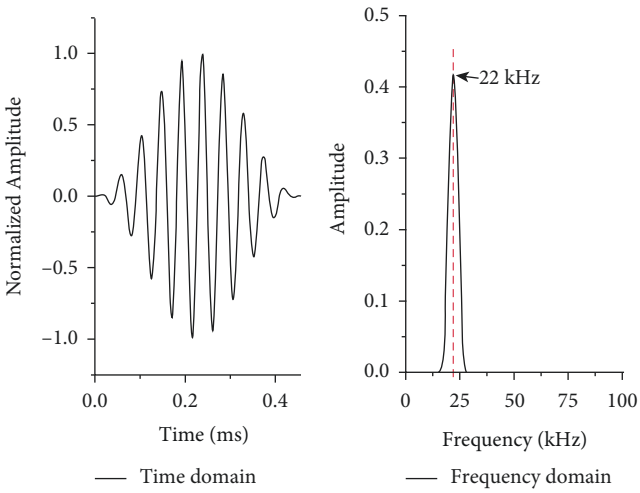

Figure 6: Time domain and frequency domain of excitation signal [33].

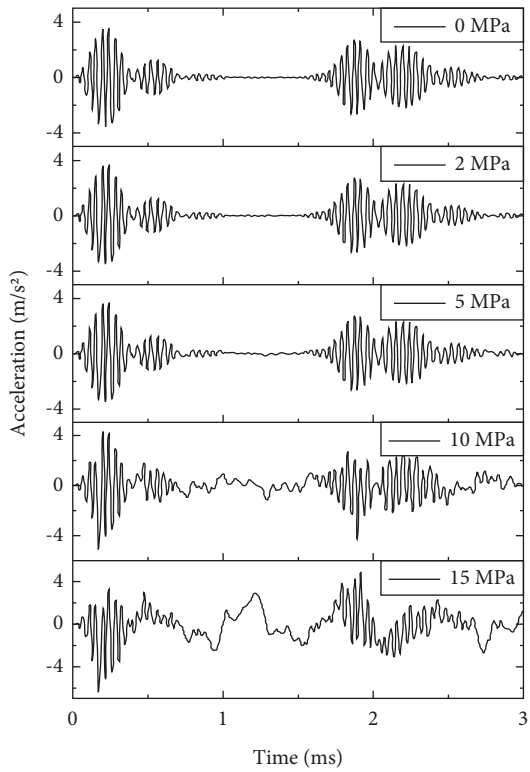

Figure 7: The influence of confining pressure on guided wave propagation in the absence of pull-out load.

cement mortar and 5 mm for the concrete are deemed adequate to obtain sufficiently accurate results. The stiffness matrix is singular when the damage value, scalar stiffness degradation, equals 1. Therefore, the maximum damage value was limited to 0.9998 to prevent the occurrence of a singular stiffness matrix [30]. The material parameters of the rockbolt, concrete, and cement mortar are presented in Table 2.

The stress of a rockbolt acting on a deep rock mass changes to 10–15 MPa during its lifetime [31, 32]. Therefore, in numerical simulations, the confining pressures of 0, 2, 5, 10, and 15 MPa are considered, which are used to analyze the influence of confining pressure on the ultrasonic guided wave propagation law and determine the bond quality of rockbolts under confining pressure. In Figure 6, the input waveform of the ultrasonic guided wave is the sine wave with 10 cycles and 22 kHz frequency obtained by the Hanning window [33].

4.1. Effect of Confining Pressure on Guided Wave Propagation without Pull-Out Load. Figure 7 displays the effect of confining pressure on ultrasonic guided wave propagation without pull-out load. As the confining pressure increases, the transmitted signal of the guided wave gradually becomes vibratory, which mainly occurs because the radial force on the rockbolt under confining pressure increases, and the guided wave propagation is restricted and becomes oscillatory. Under the confining pressures of 0, 2, and 5 MPa, the echoes of the B- and C-end received at the A-end are clearly visible, the wave packet is complete, and the effect of confining pressure is not obvious. This phenomenon is similar to the guided wave propagation law in rockbolts under a confining pressure of 2 MPa in the laboratory test. However, when the confining pressure is increased to 10 and 15 MPa, the propagation law weakens, the echo wave packet clearly oscillates, and the confining pressure becomes increasingly obvious. In the initial stage of applying the confining pressure, the concrete and cement mortar are subjected to the confining pressure, and the volume closure of the confined microcracks and cracks increases with the confining pressure. However, as the confining pressure increases, the effect of confining pressure restricts the volume change of the microcracks and cracks in the concrete and cement mortar, and the restricting effect increases with the confining pressure. With increasing confining pressure, the rockbolt and cement mortar are more closely bonded, the bonding ductility is strengthened, the radial force of the rockbolt is increased [31], and the bond quality of the rockbolt is improved. During the propagation of ultrasonic guided waves in the rockbolt, the radial vibration of the ultrasonic guided wave is restricted by the confining pressure, which causes the wave packet to oscillate but does not reduce the propagation velocity of the guided wave, which is consistent with the experimental phenomenon. Under different confining pressures, the guided waves simultaneously reach the bottom of the bond systems. According to the

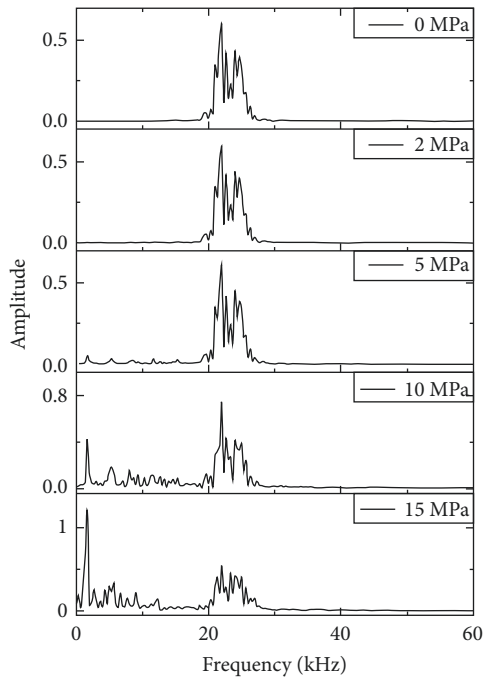

Figure 8: The change of frequency under different confining pressures.

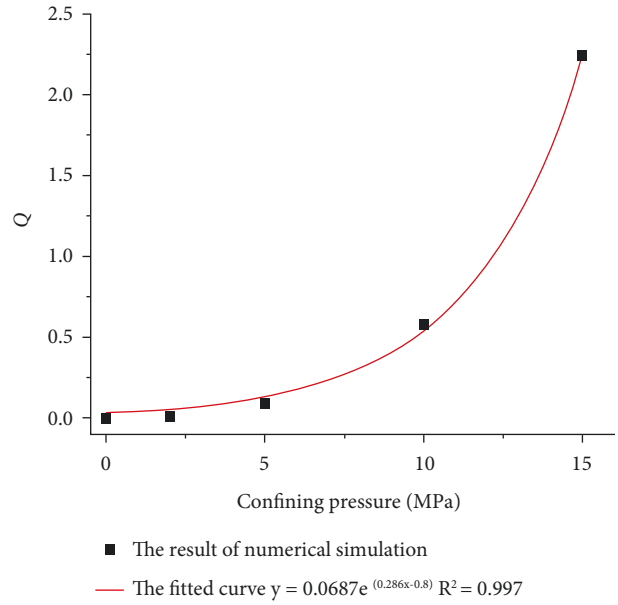

Figure 9: The relationship of Q and confining pressure without pull-out load.

above results, under no pull-out load, the weakening effect of the confining pressure on the guided wave propagation law becomes more obvious with increasing confining pressure.

The change of frequency in a guided wave under different confining pressures is shown in Figure 8. The low-frequency part of the guided wave gradually increases with the confining pressure. The relation between the Q value and confining pressure is shown in Figure 9, and the Q value exponentially increased with the confining pressure. Under low confining pressures, the Q value slowly increases. In contrast, under high confining pressures, the Q value rapidly increases, which further shows that the high-frequency part of a guided wave shifts more to the low-frequency part under high confining pressures, which weakens the propagation law of the guided wave.

4.2. Bond Quality of Rockbolts under Different Pull-Out Load and Confining Pressure. During the service period, rockbolts are frequently subjected to the interaction of the axial and radial loads. Therefore, the interaction of the pull-out load and confining pressure is mainly considered, and the propagation law of ultrasonic guided waves in grouted rockbolt systems is studied to determine the bond quality of rockbolts. Two working conditions are considered: the same pull-out load but different confining pressures and the same confining pressure but different pull-out loads.

4.2.1. Under the Same Pull-Out Load and Different Confining Pressures. Figure 10 shows the effect of confining pressure on the ultrasonic guided wave propagation under the same pull-out load. In Figure 10(a), under a pull-out load of 50 kN and confining pressure of 0 MPa, the propagation of the ultrasonic guided wave is disturbed by the pull-out load, resulting in no regularity of the guided wave propagation. When the confining pressure is increased to 5 MPa, the propagation law of the guided wave strengthens; however, the guided wave packet still oscillates, and the C-end echo can be seen. As the confining pressure is further increased, the propagation law of the ultrasonic guided wave gradually strengthens, which signifies that the existence of a large confining pressure weakens the weakening effect of the pull-out load and restrains the discreteness of guided wave propagation. In Figure 10(b), when the pull-out load is 100 kN, the guided wave propagation is irregular under the action of low confining pressure. When the confining pressure is increased from 0 to 15 MPa, the guided wave is transmitted relatively better, but there is still no regularity. Figure 10 shows that under the interaction of confining pressure and pull-out load, compared with the weakening effect of pull-out load on the propagation law of the guided wave, the confining pressure strengthens the propagation law of the guided wave. Moreover, the strengthening effect becomes more significant with increasing confining pressure. However, under the action of a large pull-out load, the strengthening effect of the confining pressure is weaker than that of the pull-out load.

Figure 11 shows the change in frequency in the guided wave with confining pressure under the action of the pull-out load. When the pull-out load is 50 kN, as the confining pressure increases, the low-frequency part in the guided wave gradually decreases, the high-frequency part increases, and the Q value exponentially decreases (as shown in Figure 12). In other words, as the confining pressure increases, the frequency in the guided wave shifts from low to high frequency. However, under a load of 100 kN, as the confining pressure increases, the high-frequency part obviously

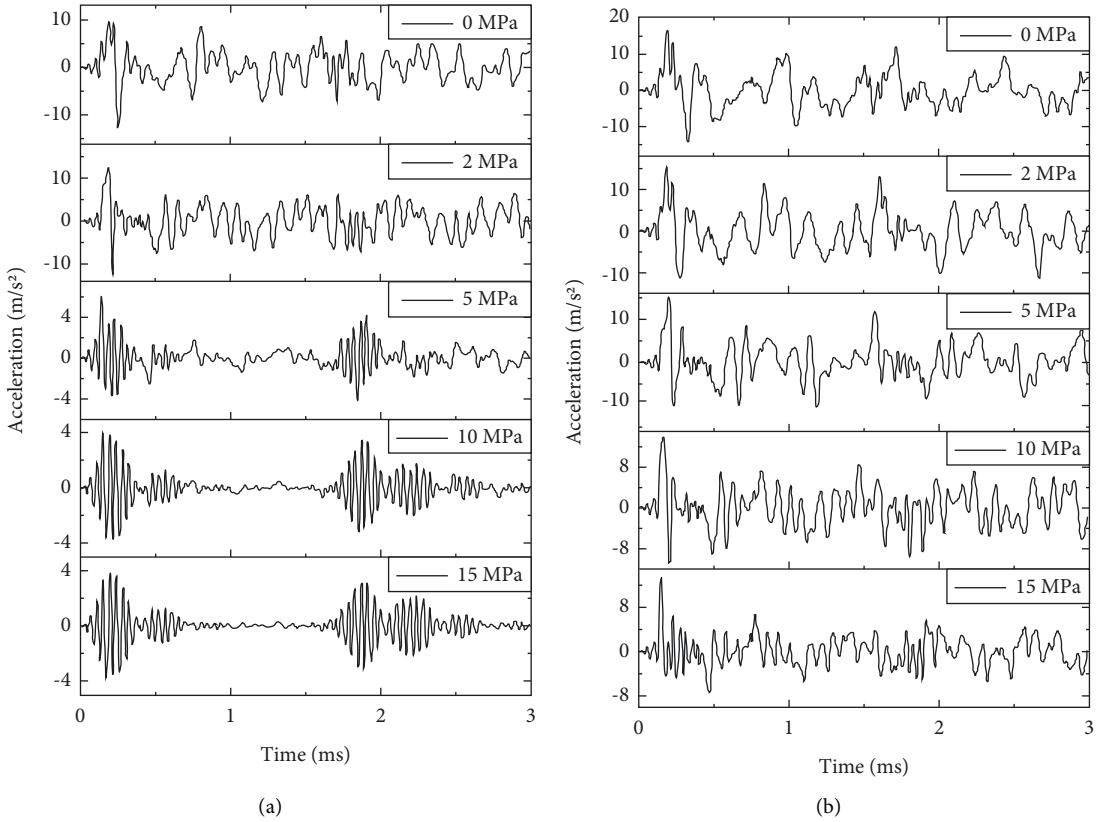

Figure 10: The influence of confining pressure on guided wave propagation under the same pull-out load. (a) 50 KN and (b) 100 KN.

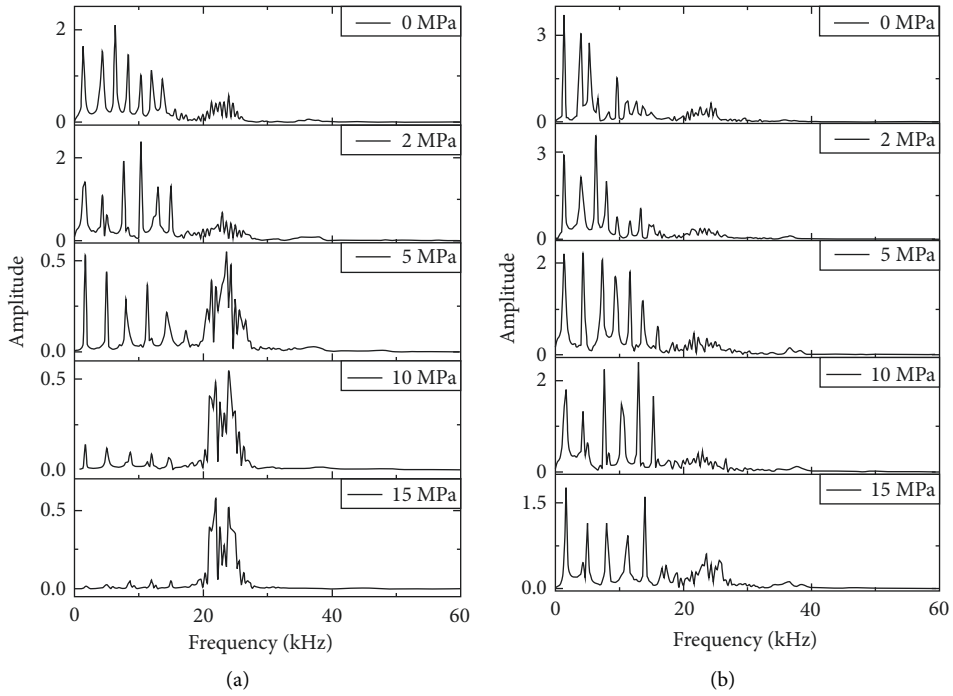

Figure 11: The change of frequency with confining pressure under pull-out load. (a) 50 KN and (b) 100 KN.

did not increase, whereas the low-frequency part decreases. Figure 12 shows that as the confining pressure increases, the Q value exponentially decreases. The frequency translation in Figure 11 reflects that the confining pressure strengthens the propagation law of the guided wave under the action of the pull-out load.

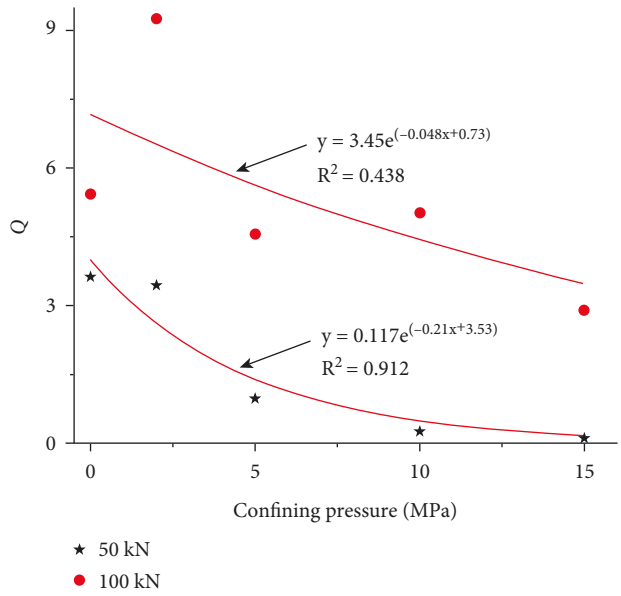

Figure 12: The relationship of Q under confining pressure and pull-out load.

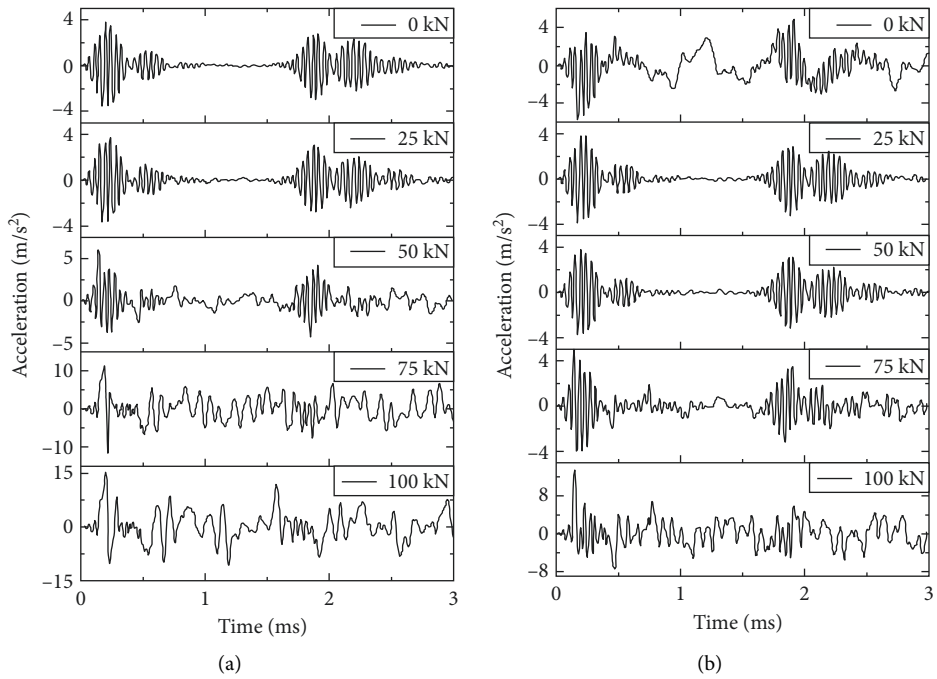

Figure 13: The influence of pull-out load on guided wave propagation under the same confining pressure. (a) 5 MPa and (b) 15 MPa.

4.2.2. Under the Same Confining Pressure and Different Pull-Out Loads. Figure 13 displays the effect of the pull-out load on the propagation of the ultrasonic guided wave under the same confining pressure. In Figure 13(a), under the same confining pressure of 5 MPa, when the pull-out load is increased to 50 kN, the propagation of the ultrasonic guided wave becomes slightly disordered, but the echo at the C-end can still be seen. Additionally, the guided wave becomes irregular under a load of 75 kN. In Figure 13(b), under a confining pressure of 15 MPa, when there is no pull-out load, the propagation law of the guided wave is very poor and the Q value is high, which is mainly due to the weakening effect of the confining pressure without a pull-out load. The propagation law of the guided wave is improved when the pull-out load increases to 25 kN, which is mainly due to the strengthening effect of the confining pressure under the pull-out load. When the pull-out load is increased to 75 kN, the guided wave propagation becomes relatively regular, but when it is increased to 100 kN, the guided wave propagation becomes irregular. Figure 13 shows that, under the same

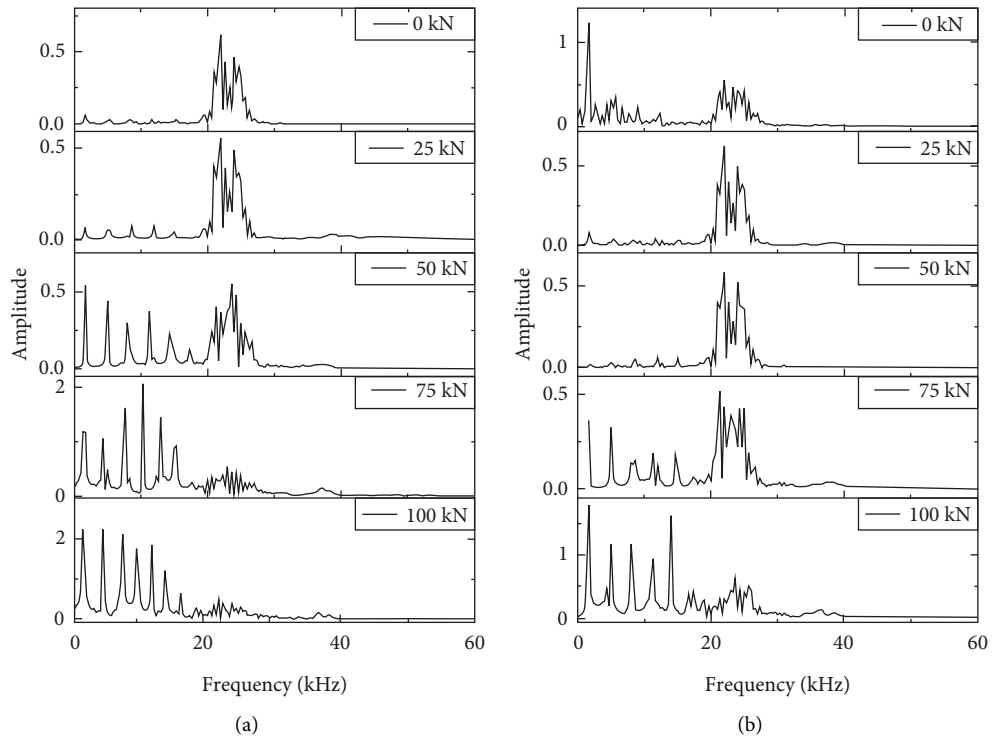

Figure 14: The change of frequency with the load under confining pressure. (a) 5 MPa and (b) 15 MPa.

confining pressure, when the pull-out load is increased, the propagation of the ultrasonic guided wave gradually becomes irregular, which signifies that the propagation of the ultrasonic guided wave is highly sensitive to the stress level. At the same pull-out load of 50 kN, the propagation law of the ultrasonic guided wave under a confining pressure of 15 MPa is better than that under a confining pressure of 5 MPa. Under the pull-out load of 75 kN, when the confining pressure is 15 MPa, the guided wave propagation has a certain regularity, and the echo of the C-end is clearly visible; however, when the confining pressure is 5 MPa, the guided wave propagation is irregular. This denotes that the confining pressure strengthens the propagation law of the guided wave. Under the same confining pressure, the guided wave cannot well diffract into the cement mortar and concrete with increasing pull-out load. Simultaneously, the existence of confining pressure restricts the radial vibration of guided waves, which causes the weakening of the regularity of guided wave propagation, and the pull-out load weakens the propagation law of ultrasonic guided waves.

Figure 14 shows the variation of frequency in the guided wave with varying pull-out load under the action of the confining pressure. Under a confining pressure of 5 MPa, the high-frequency part of the guided wave decreases with increasing pull-out load, whereas the low-frequency part increases with the pull-out load. In other words, the Q value increases in a quadratic polynomial function with increasing pull-out load (Figure 15). When the confining pressure is 5 MPa, the Q value slowly increases under a low pull-out load but rapidly increases when the pull-out load is increased from 50 to 75 kN. However, under the action of a confining

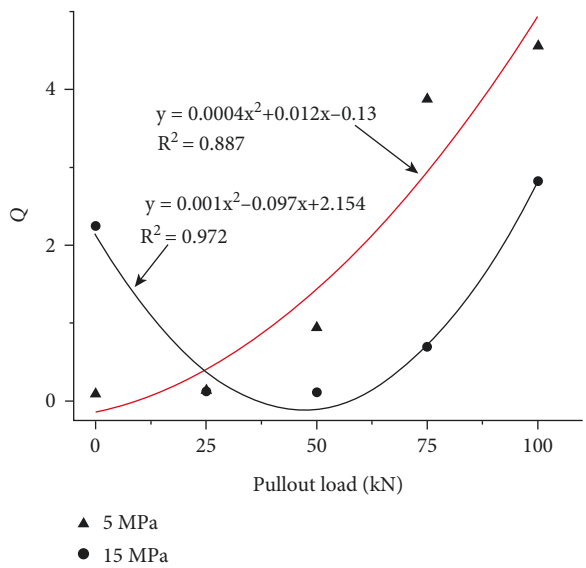

Figure 15: The relationship of Q and pull-out load under confining pressure.

pressure of 15 MPa, the confining pressure weakens the propagation law of the guided wave under no pull-out load. Thus, the low-frequency part of the guided wave frequency is very large, whereas the high-frequency part is very low, which affords a large Q value. When the pull-out load is increased, the Q value changes according to a quadratic polynomial function; that is, it first decreases and then increases.

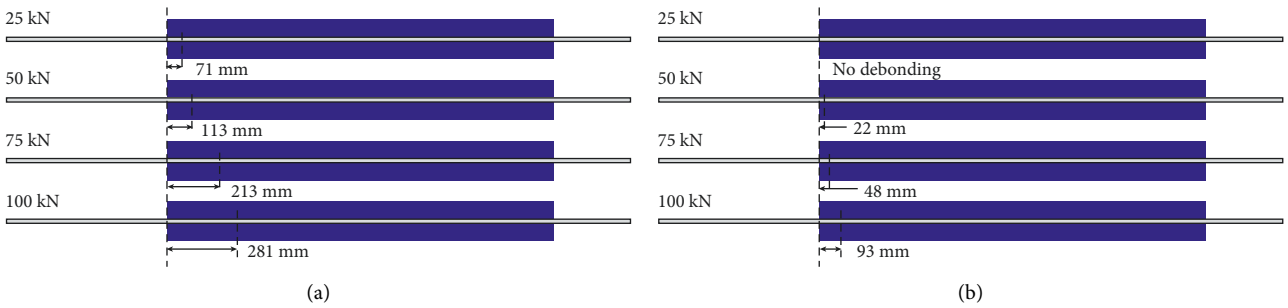

Figure 16: The rockbolt debonding status under different pull-out loads. (a) 5 MPa and (b) 15 MPa.

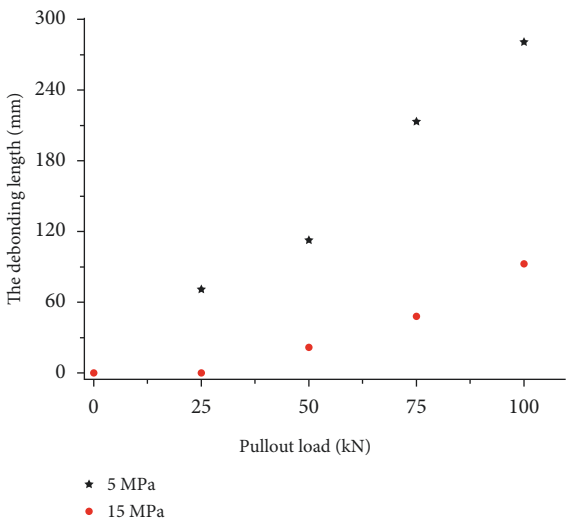

Figure 17: The rockbolt debonding length under different pull-out loads.

When the confining pressure is 5 MPa, the debonding situation of the rockbolt under different pull-out loads is shown in Figure 16(a), which displays the three-quarter model of the cylinder sample (the two-dimensional axisymmetric model was rotated around the symmetry axis to obtain the three-dimensional model in Abaqus), thus facilitating the observation of the debonding situation inside the bond system. As the load increases, the debonding length of the rockbolt increases, the bonding strength between the rockbolt and the cement mortar decreases at the front end of the anchorage body, and a gap forms between the rockbolt and the cement mortar, which causes the poor diffraction of the ultrasonic guided wave into the cement mortar and concrete at the front end of the anchorage system. However, the radial vibration of the ultrasonic guided wave in the anchor rod is limited due to the confining pressure, which causes disordered guided wave propagation. When the confining pressure is 15 MPa, the debonding of the rockbolt under different pull-out loads is shown in Figure 16(b), which also shows that the debonding length of the rockbolt increases with the load; however, the speed of increase is slower than that when the confining pressure is 5 MPa. As shown in Figure 17, with increasing pull-out load, the difference in the debonding length of the rockbolt increases. Under a 25 kN pull-out load, the rockbolt basically does not debond when the confining pressure is 15 MPa, but the rockbolt debonds for 71 mm when the confining pressure is 5 MPa. This mainly occurs due to a large amount of microcracks and crack closure in the concrete and cement mortar under high confining pressures, which strengthens the bonding strength between the rockbolt and cement mortar; that is, the rockbolt and cement mortar are more closely bonded. In Figure 16, under the same pull-out load, the debonding length of the rockbolt decreases and the bond quality of the rockbolt increases with increasing confining pressure. Under the same confining pressure, the debonding length of the rockbolt increases and the bond quality of the rockbolt decreases with increasing pull-out load.

5. Conclusions

In this study, the propagation regularity of guided waves under the combined action of confining pressure and pull-out load was experimentally and numerically studied, and the propagation regularity was then analyzed to determine the bond quality of rockbolts. The following conclusions were obtained:

(1) When there is no pull-out load, as the confining pressure increases, the closing volume of microcracks and cracks in concrete and cement mortar increases, the bonding between rockbolts and cement mortar increases, the Q value exponentially increases, the bond quality of rockbolts improves, and the propagation law of guided waves gradually weakens. Moreover, the confining pressure restricts the radial vibration of the guided wave and causes the guided wave packet to oscillate. Thus, the confining pressure has a weakening effect on the propagation law of the guided wave.

(2) Under the same pull-out load, as the confining pressure increases, the Q value exponentially decreases; that is, the low-frequency part of the guided wave frequency decreases and the high-frequency part increases. Additionally, the strengthening effect of the confining pressure on the propagation law of the guided wave and the bond quality of the rockbolt are enhanced.

(3) Under the same confining pressure, as the pull-out load increases, the Q value changes in a quadratic

polynomial function. When the confining pressure decreases, the Q value increases with the pull-out load. When the confining pressure increases, the Q value first decreases and then increases with increasing pull-out loads, and the bond quality of the rockbolt becomes poor.

This study provides the basic understanding of quantifying the bond quality based on the analysis of the guided wave propagation in the rockbolt system under the action of the confining pressure and pull-out load. Concerning the mining engineering application, the proposed method can be used to detect the bond quality of rockbolts, based on which the necessary preventive measures can be taken to ensure the stability of underground mining structures.

Data Availability

The data used to support the findings of this study are included within the article.

Conflicts of Interest

The authors declare no conflicts of interest.

Acknowledgments

This work was funded by the National Science Foundation of China (Grant no. 52104157). This support is gratefully acknowledged.

References

[1] F. Xu, K. Wang, S. G. Wang, W. W. Li, W. Q. Liu, and D. S. Du, "Experimental bond behavior of deformed rebars in half-grouted sleeve connections with insufficient grouting defect," *Construction and Building Materials*, vol. 185, pp. 264–274, 2018.

[2] Y. Cui and D. H. Zou, "Assessing the effects of insufficient rebar and missing grout in grouted rock bolts using guided ultrasonic wavesficient rebar and missing grout in grouted rock bolts using guided ultrasonic waves," *Journal of Applied Geophysics*, vol. 79, pp. 64–70, 2012.

[3] C. Q. Fang, K. Lundgren, L. G. Chen, and C. Zhu, "Corrosion influence on bond in reinforced concrete," *Cement and Concrete Research*, vol. 34, no. 11, pp. 2159–2167, 2004.

[4] F. Tondolo, "Bond behaviour with reinforcement corrosion," *Construction and Building Materials*, vol. 93, pp. 926–932, 2015.

[5] P. Craig, S. Serkan, P. Hagan et al., "Investigations into the corrosive environments contributing to premature failure of Australian coal mine rock bolts," *International Journal of Mining Science and Technology*, vol. 26, no. 1, pp. 59–64, 2016.

[6] L. P. Srivastava and M. Singh, "Effect of fully grouted passive bolts on joint shear strength parameters in a blocky mass," *Rock Mechanics and Rock Engineering*, vol. 48, no. 3, pp. 1197–1206, 2015.

[7] M. Ghadimi, K. Shahriar, and H. Jalalifar, "A new analytical solution for the displacement of fully grouted rock bolt in rock joints and experimental and numerical verifications," *Tunnelling and Underground Space Technology*, vol. 50, pp. 143–151, 2015.

[8] W. Nie, Z. Y. Zhao, S. Q. Ma, and W. Guo, "Effects of joints on the reinforced rock units of fully-grouted rockbolts," *Tunnelling and Underground Space Technology*, vol. 71, pp. 15–26, 2018.

[9] D. S. Zou, J. L. Cheng, R. J. Yue, and X. Y. Sun, "Grout quality and its impact on guided ultrasonic waves in grouted rock bolts," *Journal of Applied Geophysics*, vol. 72, no. 2, pp. 102–106, 2010.

[10] V. Madenga, D. H. Zou, and C. Zhang, "Effects of curing time and frequency on ultrasonic wave velocity in grouted rock bolts," *Journal of Applied Geophysics*, vol. 59, no. 1, pp. 79–87, 2006.

[11] I. M. Lee, S. I. Han, H. J. Kim, J. D. Yu, B. K. Min, and J. S. Lee, "Evaluation of rock bolt integrity using Fourier and wavelet transforms," *Tunnelling and Underground Space Technology*, vol. 28, pp. 304–314, 2012.

[12] J. D. Yu, Y. H. Hong, Y. H. Byun, and J. S. Lee, "Non-destructive evaluation of the grouted ratio of a pipe roof support system in tunneling," *Tunnelling and Underground Space Technology*, vol. 56, pp. 1–11, 2016.

[13] M. D. Beard and M. J. S. Lowe, "Non-destructive testing of rock bolts using guided ultrasonic waves," *International Journal of Rock Mechanics and Mining Sciences*, vol. 40, no. 4, pp. 527–536, 2003.

[14] Y. Cui and D. H. Zou, "Numerical simulation of attenuation and group velocity of guided ultrasonic wave in grouted rock bolts," *Journal of Applied Geophysics*, vol. 59, no. 4, pp. 337–344, 2006.

[15] C. Cao, T. Ren, and C. Chris, "Introducing aggregate into grouting material and its influence on load transfer of the rock bolting system," *International Journal of Mining Science and Technology*, vol. 24, no. 3, pp. 325–328, 2014.

[16] P. Rizzo, "Ultrasonic wave propagation in progressively loaded multi-wire strands," *Experimental Mechanics*, vol. 46, no. 3, pp. 297–306, 2006.

[17] F. Chen and P. D. Wilcox, "The effect of load on guided wave propagation," *Ultrasonics*, vol. 47, no. 1-4, pp. 111–122, 2007.

[18] H. Kwun, K. A. Bartels, and J. J. Hanley, "Effects of tensile loading on the properties of elastic-wave propagation in a strand," *Journal of the Acoustical Society of America*, vol. 103, no. 6, pp. 3370–3375, 1998.

[19] H. L. R. Chen and K. Wissawapaisal, "Measurement of tensile forces in a seven-wire prestressing strand using stress waves," *Journal of Engineering Mechanics*, vol. 127, no. 6, pp. 599–606, 2001.

[20] H. L. R. Chen and K. Wissawapaisal, "Application of wigner-ville transform to evaluate tensile forces in seven-wire prestressing strands," *Journal of Engineering Mechanics*, vol. 128, no. 11, pp. 1206–1214, 2002.

[21] X. C. Liu, B. Wu, F. Qin, C. F. He, and Q. Han, "Observation of ultrasonic guided wave propagation behaviours in prestressed multi-wire structures," *Ultrasonics*, vol. 73, pp. 196–205, 2017.

[22] S. S. Yu, W. C. Zhu, L. L. Niu, S. C. Zhou, and P. H. Kang, "Experimental and numerical analysis of fully-grouted long rockbolt load-transfer behavior," *Tunnelling and Underground Space Technology*, vol. 85, pp. 56–66, 2019.

[23] K. S. Fan, B. H. Shen, S. W. Liu, and J. K. Jiao, "Numerical test and application of propagation characteristics of stress wave on roadway roof anchored body," *Journal of Mining and Safety Engineering*, vol. 28, no. 4, pp. 245–253, 2018, In Chinese.

[24] J. G. Chen and Y. X. Zhang, "Analysis on characteristics of dynamic signal for bolt anchorage system," *Chinese Journal of Geotechnical Engineering*, vol. 30, no. 7, pp. 1051–1057, 2008, In Chinese.

[25] X. Fu, R. X. Fu, W. P. Wang, and Q. X. Luo, "Testing grouted quality in prestressed duct with impact-echo method," *Construction Technology*, vol. 32, no. 11, pp. 37-38, 2003, In Chinese.

[26] J. Lee and G. L. Fenves, "Plastic-damage model for cyclic loading of concrete structures," *Journal of Engineering Mechanics*, vol. 124, no. 8, pp. 892–900, 1998.

[27] Dassault Systemes Simulia, *ABAQUS Theory Manual & Users Manuals Version 6.11*, Simulia, Rhode Island, USA, 2014.

[28] J. Henriques, L. Simões da Silva, and I. B. Valente, "Numerical modeling of composite beam to reinforced concrete wall joints part1: calibration of joint components," *Engineering Structures*, vol. 52, pp. 747–761, 2013.

[29] J. Henriques, F. Gentili, L. Simões da Silva, and R. Simoes, "Component based design model for composite beam to reinforced concrete wall moment-resistant joints," *Engineering Structures*, vol. 87, pp. 86–104, 2015.

[30] W. R. Yang, X. J. He, and L. Dai, "Damage behaviour of concrete beams reinforced with GFRP bars," *Composite Structures*, vol. 161, pp. 173–186, 2017.

[31] L. S. Lv, H. F. Yang, T. B. Zhang, and Z. H. Deng, "Bond behavior between recycled aggregate concrete and deformed bars under uniaxial lateral pressure," *Construction and Building Materials*, vol. 185, pp. 12–19, 2018.

[32] L. B. Martin, M. Tijani, F. H. Hassen, and A. Noiret, "Assessment of the bolt-grout interface behavior of fully grouted rockbolts from laboratory experiments under axial loads," *International Journal of Rock Mechanics and Mining Sciences*, vol. 63, pp. 50–61, 2013.

[33] S. S. Yu, W. C. Zhu, and L. L. Niu, "Experimental and numerical evaluation on debonding of fully grouted rockbolt under pull-out loading," *International Journal of Coal Science & Technology*, vol. 9, no. 1, 2022.